THE JOURNAL OF PHYSICAL CHEMISTRY B

Article

pubs.acs.org/JPCB

Singlet-Oxygen-Mediated Cell Death Using Spatially-Localized Two-Photon Excitation of an Extracellular Sensitizer

Frederico M. Pimenta,[†] Rasmus L. Jensen,[†] Lotte Holmegaard,[†] Tatiana V. Esipova,[‡] Michael Westberg,[†] Thomas Breitenbach,[†] and Peter R. Ogilby*,[†]

[†]Center for Oxygen Microscopy and Imaging, Department of Chemistry, Aarhus University, Aarhus 8000, Denmark

[‡]Department of Biochemistry and Biophysics, University of Pennsylvania, Philadelphia, Pennsylvania 19104, United States

ABSTRACT: Controlling and quantifying the photosensitized production of singlet oxygen are key aspects in mechanistic studies of oxygen-dependent photoinitiated cell death. In this regard, the commonly accepted practice of using intracellular photosensitizers is, unfortunately, plagued by problems that include the inability to accurately (1) quantify the sensitizer concentration in the irradiated domain and (2) control the local environment that influences light delivery and sensitizer photophysics. However, capitalizing on the fact that singlet oxygen produced outside a cell is also cytotoxic, many of these problems can be avoided with the use of an extracellular sensitizer. For the present study, a hydrophilic dendrimer-encased membrane-impermeable sensitizer was used to generate an extracellular population of singlet oxygen upon spatially localized two-photon irradiation. Through the use of this sensitizer and this approach, it is now possible to better control the singlet oxygen dose in microscope-based time- and space-resolved single cell experiments. Thus, we provide a solution to a limiting problem in mechanistic studies of singlet-oxygen-mediated cell death.

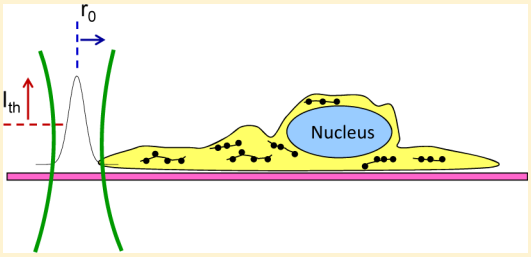

INTRODUCTION

Singlet oxygen, $O_2(a^1\Delta_g)$, is the lowest excited electronic state of molecular oxygen. It has a unique chemistry that results in the oxygenation of many organic molecules.[1] In this way, $O_2(a^1\Delta_g)$ plays important roles in biology; among other things, it is involved in mechanisms of signaling and death in mammalian cells.[2−6]

$O_2(a^1\Delta_g)$ can be produced in a photosensitized process wherein light is absorbed by a given molecule (the sensitizer) followed by energy transfer from the excited state sensitizer to ground state oxygen, $O_2(X^3\Sigma_g^-)$ (Figure 1).[2,7] The production of $O_2(a^1\Delta_g)$ in this way is a natural phenomenon (i.e., we live in a world of light, oxygen, and molecules that can photosensitize the production of $O_2(a^1\Delta_g)$). The photosensitized production of $O_2(a^1\Delta_g)$ is also used as a clinical tool to destroy/remove cells and alter tissue (e.g., photodynamic cancer treatments,[4,6] treating age-related macular degeneration,[8] and altering corneal properties[9]).

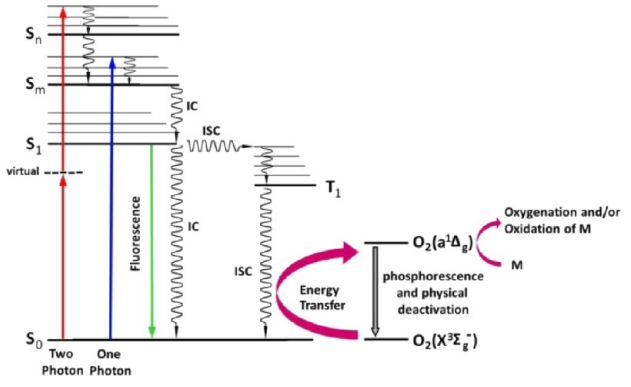

Figure 1. Diagram illustrating the one- and two-photon triplet state photosensitized production of $O_2(a^1\Delta_g)$. S denotes a sensitizer singlet state, T a triplet state, ISC intersystem crossing, and IC internal conversion.

Over the years, sensitizer excitation and $O_2(a^1\Delta_g)$ production have traditionally been achieved in a one-photon process wherein the energy of an incident photon is resonant with a transition in the sensitizer (Figure 1).[7] However, when the incident photon flux is large (i.e., in a focused laser beam), sensitizer excitation and $O_2(a^1\Delta_g)$ production can also occur via the simultaneous absorption of two low-energy photons that, by themselves, are not resonant with a transition in the sensitizing molecule (Figure 1).[2] This latter process has distinct advantages with respect to the spatial localization and confinement of the excited states produced[10−13] and can likewise result in cell death and tissue damage.[10,14,15]

The mechanisms of photoinitiated $O_2(a^1\Delta_g)$-mediated processes in cells are complicated and still poorly understood, certainly with respect to cell signaling and cell death. Drawbacks in elucidating these mechanisms are often traced to the difficulties associated with controlling and quantifying the amount of $O_2(a^1\Delta_g)$ produced in a specific domain in or near a cell.[16]

Received: May 22, 2012
Revised: July 25, 2012
Published: August 2, 2012

dx.doi.org/10.1021/jp304954m | J. Phys. Chem. B 2012, 116, 10234−10246

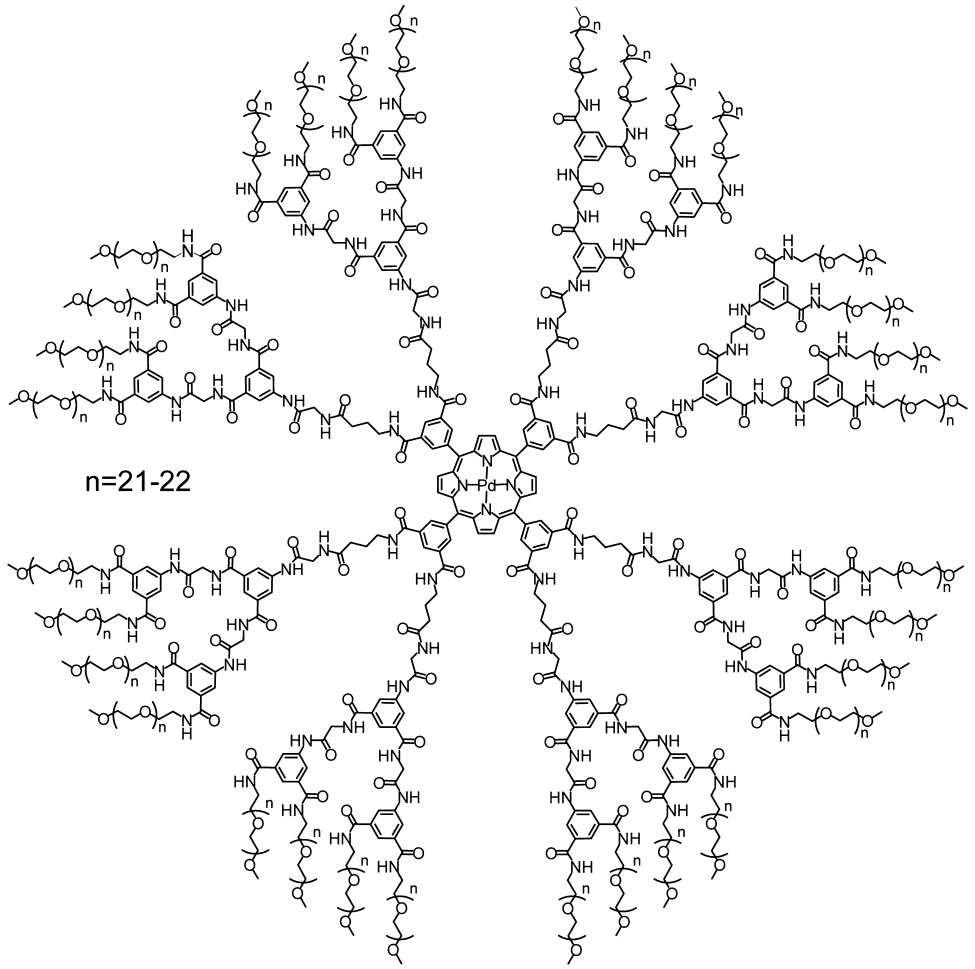

Figure 2. Structure of the poly(ethylene glycol)-coated dendrimer-encased Pd porphyrin (PD1) used as the extracellular $O_2(a^1\Delta_g)$ sensitizer in this study.

When using an intracellular sensitizer, it is unfortunately difficult to establish and quantify its concentration.[17] This is particularly true with the common practice in which sensitizer incorporation is achieved by incubating the cell in a medium containing either the sensitizer itself or a biological precursor of the sensitizer.[17] Moreover, it is difficult to maintain a constant and reproducible environment around the sensitizer, particularly under conditions in which the cell is being perturbed by the $O_2(a^1\Delta_g)$ thus produced.[17−19] Changes in the local environment of the sensitizer, including the redistribution of the sensitizer in the cell, can influence light absorption and the subsequent efficiency of $O_2(a^1\Delta_g)$ production. Finally, because of the inhomogeneous environment inside a cell with domains that have a different refractive index, scattering of the incident light plays a significant role in determining the number of photons actually absorbed by a sensitizer in a given intracellular domain.[10] Combined, all of these factors make it difficult to control $O_2(a^1\Delta_g)$ production inside a cell, even if only precise relative measurements are desired.

By using an extracellular sensitizer, one can avoid many of the environment-dependent problems outlined above. Of course, the key prerequisite in this regard is that the extracellular $O_2(a^1\Delta_g)$ thus produced must be cytotoxic. Fortunately, as with the use of intracellular sensitizers, conditions can be chosen such that this is indeed the case.[20] Admittedly, the processes that lead to cell death are likely different for an extracellular population of $O_2(a^1\Delta_g)$ than for an intracellular population of $O_2(a^1\Delta_g)$.[5,21] Specifically, the initial targets of $O_2(a^1\Delta_g)$, and the processes that subsequently ensue, are likely to be different. Nevertheless, as we establish in the current work, the use of an extracellular sensitizer can provide a much-needed standard from which subsequent studies can propagate.

Our present study was performed using a dendrimer-encased membrane-impermeable sensitizer with mammalian cells (i.e., HeLa cancer cells) and is characterized by three key aspects: (1) $O_2(a^1\Delta_g)$ is made exclusively in the extracellular medium where it is much easier to exert control over parameters that influence light absorption, (2) the environment immediately surrounding the sensitizer does not change during the experiment, thus facilitating constant light absorption and $O_2(a^1\Delta_g)$ production, and (3) $O_2(a^1\Delta_g)$ is made through a two-photon sensitized process that facilitates spatial localization of the excitation volume. Thus, we present a method by which a controlled dose of cytotoxic $O_2(a^1\Delta_g)$ can be readily produced in single cell experiments, which, in turn, should facilitate more informative imaging-based mechanistic studies of $O_2(a^1\Delta_g)$-mediated cell death.

EXPERIMENTAL SECTION

Chemicals. The poly(ethylene glycol)-coated, dendrimer-encased palladium porphyrin (Figure 2), denoted PD1,[22] the 2-

Table 1. Decay Constants of the PD1 Triplet State in the Absence, $(k_T^{N2})^{-1}$, and Presence, $(k_{T1})^{-1}$ and $(k_{T2})^{-1}$, of Oxygen, the $O_2(a^1\Delta_g)$ Lifetime, τ_Δ, the Fraction of PD1 Triplet States Quenched by Oxygen, f_T, and the PD1-Sensitized $O_2(a^1\Delta_g)$ Quantum Yield, ϕ_Δ, under a Variety of Conditions[a]

conditions	$(k_T^{N2})^{-1}$ (μs)	$(k_{T1})^{-1}$ (μs) (A_1)[b]	$(k_{T2})^{-1}$ (μs) (A_2)[b]	τ_Δ (μs)	f_T	ϕ_Δ
6.2 °C/air	947 ± 3	71 ± 6 (0.28)	197 ± 5 (0.72)	76.4 ± 0.8	0.83 ± 0.06	0.81 ± 0.06
21.2 °C/air	886 ± 2	24 ± 2 (0.22)	102 ± 1 (0.78)	68.8 ± 0.7	0.90 ± 0.06	0.88 ± 0.06
38.2 °C/air	813 ± 3	14 ± 1 (0.23)	54 ± 1 (0.77)	61.4 ± 0.6	0.94 ± 0.07	0.92 ± 0.07
55.7 °C/O_2	710 ± 2	2.0 ± 0.2 (0.38)	8.3 ± 0.5 (0.62)	55.6 ± 0.5	0.99 ± 0.07	0.99 ± 0.07

[a]Data were recorded in a D_2O-based phosphate buffer solution at pH 7.4. [b]Weighting factors obtained from biexponential fit to the data (i.e., $A_1 \exp(-k_{T1}t) + A_2 \exp(-k_{T2}t)$).

sulfonic acid derivative of phenalenone,[23] and 2,5-dibromo-1,4-bis(2-(4-diphenyl-aminophenyl)vinyl)-benzene[24] were synthesized as described in the references cited. D_2O (99% D) was obtained from EurisoTop, and the Alexa Fluor 680 Annexin V conjugate was obtained from Molecular Probes/Invitrogen. All other chemicals were obtained from Sigma-Aldrich and used as received.

Cells. The preparation of HeLa cells and the description of our standard maintenance medium (SMM) have been published.[10,18,25] For the present study, cells were cultured in a growth medium that contained 10% fetal calf serum and 1% antibiotics. However, for the kinetic experiments performed in a growth medium, the cultured cells were first rinsed and then covered with a growth medium that did not have the serum and antibiotics. This latter growth medium was prepared using the Minimum Essential Medium (MEM) Powder supplied by Sigma-Aldrich. In this way, we could readily prepare both H_2O- and D_2O-based solutions. Our media consisted of 9.3 mg/mL MEM, 2.2 mg/mL sodium bicarbonate, and 0.29 mg/mL L-glutamine. The water for the growth media was sterilized by filtration (0.2 μm filter).

On the microscope stage, the cells were housed in an incubator (Okolab CO2 Electric Microscope Stage Incubator) with controlled temperature (37 °C) and atmosphere (5% CO_2, 95% air). The gases were warmed in a temperature-controlled humidifying module before being introduced into the stage incubator. The stage incubator was allowed to stabilize for 30 min before cells were introduced.

The imaging-based experiments to demonstrate that PD1 remains in the extracellular medium were carried out as described previously for a related dendrimer-encased Pd porphyrin.[20] Experiments were also performed to indicate that PD1 does not associate with the cell membrane: upon exposure of the cell to PD1 and then washing the cell with a PD1-free medium, irradiation centered at 400 nm (i.e., one-photon excitation of PD1) did not adversely affect the cell over the pertinent time course of our experiments.

The procedure used for the Annexin assay differed slightly from that used in our earlier studies.[10] In the present study, the Annexin conjugate was present in the medium during the period in which PD1 was irradiated. The Alexa Fluor 680 Annexin conjugate was chosen for this specific reason; its absorption spectrum does not overlap with that of PD1. In this way, we can continually monitor cell response upon irradiation. A drawback of this approach is that we also stain "dirt" in our sample (e.g., membrane waste released by the cells), and this gives rise to a comparatively high background signal that would otherwise be absent in samples that had been washed before the addition of the Annexin conjugate. In the Annexin assay, excitation was achieved through a 655 nm (40 nm full-width at half-maximum (fwhm)) bandpass filter, and emission was detected through a 715 nm (40 nm fwhm) bandpass filter.

The effect of the medium on cell survival in the absence of PD1 irradiation was likewise assessed using the Annexin V assay. Thus, for D_2O-based SMM, for example, we started to see a positive Annexin stain in some cells after an incubation period of 2−3 h.

Instrumentation and Approach. The femtosecond laser system and the approach used to quantify both $O_2(a^1\Delta_g)$ yields and two-photon absorption cross-sections are described in published articles.[26,27] It is important to note that these measurements were not made using microscope optics and focused beams. Rather, the incident light was a collimated beam (diameter ≈ 2 mm) that propagated through the sample in a 1 cm cuvette. Under all conditions, the sample absorbance was low; therefore, the emitted light that was detected originated from a homogeneous spatial domain.

For the $O_2(a^1\Delta_g)$ quantum yield studies, the integrated intensities of the $O_2(a^1\Delta_g) \rightarrow O_2(X^3\Sigma_g^-)$ signals were normalized by the $O_2(a^1\Delta_g)$ lifetimes recorded in the respective experiments.[28] The 2-sulfonic acid derivative of phenalenone was used as the standard ($\phi_\Delta = 0.97 \pm 0.06$).[29] One advantage of using this molecule as a standard is that, with a ϕ_Δ value of unity, we can be reasonably secure with the assumption that ϕ_Δ for this standard will be independent of temperature over the range examined in our study. This assumption is substantiated by the fact that, at all temperatures, the independently determined value of f_T for PD1 equals ϕ_Δ determined for PD1 (Table 1). The concentration of PD1 used for these in vitro photophysical studies was 4.0×10^{-7} M (i.e., sample absorbance at 420 nm was ∼0.1).

For the two-photon absorption cross-section experiments in which the intensity of PD1 phosphorescence was compared to the intensity of $O_2(a^1\Delta_g)$ phosphorescence sensitized by the two-photon reference standard, it was necessary to independently determine the quantum yield of PD1 phosphorescence, ϕ_p, in air-saturated D_2O at 21 °C (i.e., the two-photon cross-section measurements were performed in air-saturated D_2O). This was done using fluorescein in alkaline H_2O as a standard ($\phi_F = 0.92 \pm 0.02$),[30,31] yielding $\phi_p = 0.0031 \pm 0.0005$ for PD1. Note that this value of ϕ_p is ∼10× less than that reported for PD1 in an argon-saturated solution[22] and thus is consistent with the value of $f_T = 0.9$ reported in Table 1. Two-photon measurements were performed using a laser repetition rate of 1 kHz and average powers at the sample that covered the range of 5−12 mW

For the cell kill experiments, the 820 nm (fwhm = 12 nm) output of a different femtosecond laser operating at 80 MHz (Mai Tai from Spectra Physics) was coupled onto a microscope objective (60× Olympus LUMPlanFI/IR, water immersion, NA 0.9) in an inverted microscope (Olympus IX71), as previously

described for related systems.[10,11,18] The power incident on the objective was adjusted using a combination of a half-wave plate and a Glan-Taylor polarizer.[26] The power was also measured at the microscope stage (Thorlabs S120VC power meter), and the values obtained were consistent with what is expected given the transmittance of the optics in the microscope. Images of the cells were obtained using a CCD camera (Evolution QEi Fast-Cooled Mono 12 bit camera from QI Imaging). Bright field illumination was achieved through a 660 nm (fwhm = 10 nm) band-pass filter.

RESULTS AND DISCUSSION

Membrane-Impermeable Extracellular Sensitizer. PD1 was originally developed as a phosphorescent probe for ground state oxygen.[22] Under the conditions and incident light doses typically used for oxygen detection and imaging in cell cultures or in vivo, these encased porphyrins are not toxic.[32] However, they sensitize the production of $O_2(a^1\Delta_g)$ and can induce cell death when present at higher concentrations and when subjected to light doses that significantly exceed those required for oxygen imaging.[20]

PD1 has the particularly pertinent characteristic that, when exposed to HeLa cells, it does not associate with, nor does it enter, the cell; it remains in the extracellular medium. This is true even under conditions where exposure of the cell to $O_2(a^1\Delta_g)$ might begin to adversely affect the integrity of the cell membrane. This property of PD1 was verified by monitoring the 700 nm phosphorescence of PD1 in imaging-based experiments, as described previously for a related dendrimer-encased porphyrin.[20] Although not explicitly tested, we assume this feature of PD1 also extends to mammalian cells other than HeLa cells.

Unlike other dendrimer-encased systems,[20,33] PD1 is readily handled in aqueous solutions and does not aggregate. Moreover, the porphyrin in PD1 does not photobleach upon irradiation under the conditions used herein to initiate cell death. This likely reflects the fact that, once generated, $O_2(a^1\Delta_g)$ diffuses away from the porphyrin and the dendrimer-determined probability for re-encounter is small; an interpretation that is consistent with our independent study of $O_2(a^1\Delta_g)$ quenching by PD1 (vide infra). Likewise, the dendritic branches themselves do not react with $O_2(a^1\Delta_g)$,[20] and thus, the immediate environment of the porphyrin does not change during an experiment. The experiments to confirm this latter point are a corollary to those used to establish that the porphyrin itself is photostable; the intensity and decay kinetics of PD1 phosphorescence do not change upon prolonged irradiation in an oxygen-containing solution. This photostability is particularly pertinent for two-photon excitation where subtle changes in the local environment of the chromophore can appreciably influence the probability of light absorption and $O_2(a^1\Delta_g)$ production.[34] Finally, under the microscope-based, single cell conditions employed herein, where equilibration with a $O_2(X^3\Sigma_g^-)$-containing atmosphere is facile, a reaction-dependent depletion of $O_2(X^3\Sigma_g^-)$ in the system will not occur. This ensures that the rate and efficiency of sensitized $O_2(a^1\Delta_g)$ production will indeed remain constant during the period of PD1 irradiation.

On the basis of this information, coupled with the fact that extracellular $O_2(a^1\Delta_g)$ can indeed be cytotoxic,[20] we set out to further explore the possibility of using PD1 to establish a dosimetry standard for photosensitized $O_2(a^1\Delta_g)$-mediated cell death.

Photosensitized Singlet Oxygen Production. To establish a dosimetry standard, we must quantify the kinetics and yield of photosensitized $O_2(a^1\Delta_g)$ production. This is particularly pertinent in the case of PD1 since oxygen diffusion through the coated dendrimer to reach the sensitizer can be comparatively slow,[22] and this will influence the pertinent $O_2(a^1\Delta_g)$ parameters.

The lifetime of the PD1 S_1 state is sufficiently short as to preclude quenching by $O_2(X^3\Sigma_g^-)$, and $S_1 \rightarrow T_1$ intersystem crossing is sufficiently efficient that the only precursor for the sensitized production of $O_2(a^1\Delta_g)$ is the PD1 T_1 state. Under these conditions, we can express the quantum yield of $O_2(a^1\Delta_g)$ production, ϕ_Δ, as a product of three terms: the quantum yield of T_1 production, ϕ_T; the fraction of T_1 states quenched by $O_2(X^3\Sigma_g^-)$, f_T; and the fraction of the $T_1-O_2(X^3\Sigma_g^-)$ interactions that yield $O_2(a^1\Delta_g)$, S_Δ (eq 1). With respect to the latter term, $S_\Delta < 1.0$ is observed for many sensitizers, reflecting the fact that energy transfer to form $O_2(a^1\Delta_g)$ is not a prerequisite in the process whereby $O_2(X^3\Sigma_g^-)$ induces the $T_1 \rightarrow S_0$ transition.[7,35,36]

$$\phi_\Delta = \phi_T f_T S_\Delta \quad (1)$$

Quantum Yield, ϕ_Δ, of $O_2(a^1\Delta_g)$ Sensitized by PD1. The quantum yield of PD1-sensitized $O_2(a^1\Delta_g)$ production was determined by recording the integrated intensity of the time-resolved $O_2(a^1\Delta_g) \rightarrow O_2(X^3\Sigma_g^-)$ phosphorescence signal at 1275 nm and comparing it to the integrated intensity of the $O_2(a^1\Delta_g) \rightarrow O_2(X^3\Sigma_g^-)$ phosphorescence signal obtained from a reference standard for which ϕ_Δ is known.[28,37] The standard used was the 2-sulfonic acid derivative of phenalenone (ϕ_Δ = 0.97 ± 0.06).[29] The ϕ_Δ values thus obtained indicate that PD1 is a very efficient source of $O_2(a^1\Delta_g)$ (Table 1).

Lifetime of $O_2(a^1\Delta_g)$, τ_Δ, Sensitized by PD1. As shown in Figure 3, the evolution in time of a T_1-sensitized $O_2(a^1\Delta_g) \rightarrow O_2(X^3\Sigma_g^-)$ phosphorescence signal is described as a difference of two exponential functions (i.e., the signal will first rise and then fall).[2,38] In cases where the rate constant for $O_2(a^1\Delta_g)$ removal, k_Δ, is much smaller than the rate constant for the decay of the $O_2(a^1\Delta_g)$ precursor, k_T, then the lifetime of $O_2(a^1\Delta_g)$, $\tau_\Delta = 1/k_\Delta$, is readily obtained from the falling portion of the time-resolved 1275 nm $O_2(a^1\Delta_g)$ phosphorescence signal. For aqueous systems, the inequality $k_\Delta < k_T$ can generally be achieved by replacing H_2O with D_2O, exploiting the fact that $k_\Delta(D_2O)$ is ~20× smaller than $k_\Delta(H_2O)$ [i.e., τ_Δ in H_2O is ~3.5 μs, whereas τ_Δ in D_2O is ~68 μs].[39] However, for our present case of PD1-sensitized $O_2(a^1\Delta_g)$ production, the overall rate constant for T_1 decay, k_T, is comparatively small due to the slow dendrimer-mediated diffusion-dependent term for $O_2(X^3\Sigma_g^-)$-induced T_1 deactivation. Thus, $k_\Delta \approx k_T$ and/or $k_\Delta > k_T$, depending on the specific experimental conditions, and it becomes necessary to independently quantify k_T to accurately extract the desired value of k_Δ from the 1275 nm $O_2(a^1\Delta_g)$ phosphorescence signal.

We quantified k_T by monitoring PD1 phosphorescence at 700 nm in time-resolved experiments (Figure 4). To complement the $O_2(a^1\Delta_g)$ phosphorescence experiments, data were recorded at different oxygen concentrations and different temperatures in a D_2O-based phosphate buffer solution at pH 7.4. The rate of PD1 T_1 deactivation by $O_2(X^3\Sigma_g^-)$ increased with an increase in both the concentration of dissolved oxygen and in the sample temperature, as expected. Most importantly, however, T_1 decay did not follow first-order kinetics and could not be fitted with a single exponential function (i.e., $\exp(-k_T t)$)

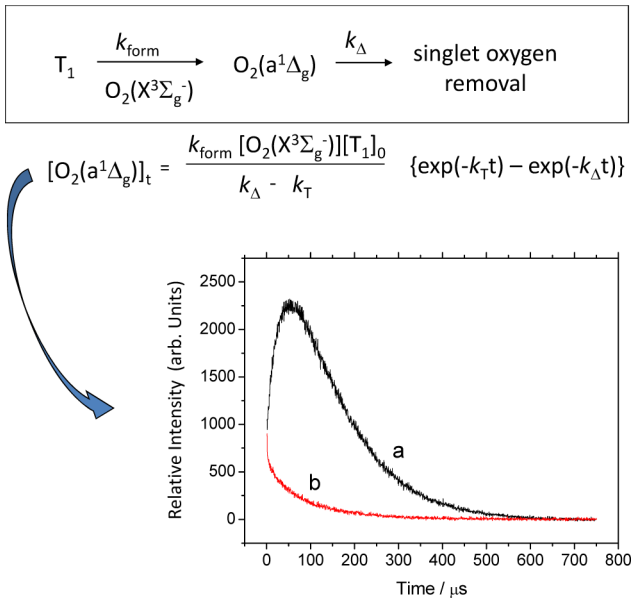

Figure 3. (top) Kinetic scheme for the T_1-sensitized production and subsequent removal of $O_2(a^1\Delta_g)$. (middle) Equation based on this kinetic scheme that shows how the concentration of $O_2(a^1\Delta_g)$ will evolve in time, *t*, upon the rapid production of T_1 in a pulsed laser experiment.[38] The first-order rate constant k_T represents all channels by which T_1 is removed, including processes that do not result in $O_2(a^1\Delta_g)$ formation, and $[T_1]_0$ represents the T_1 concentration at t = 0. At any given time *t*, the concentration of $O_2(a^1\Delta_g)$ is proportional to the intensity of $O_2(a^1\Delta_g)$ phosphorescence. (bottom) (a) $O_2(a^1\Delta_g)$ phosphorescence signal observed from a 21 °C PD1-sensitized experiment in a D_2O-based phosphate buffer solution at pH 7.4; (b) 1275 nm emission signal observed upon irradiation of PD1 in a D_2O-based phosphate buffer solution containing 2 mM BSA. The latter quenches all of the $O_2(a^1\Delta_g)$ produced by PD1, and this signal is thus assigned to PD1 phosphorescence transmitted through the 1275 nm interference filter.

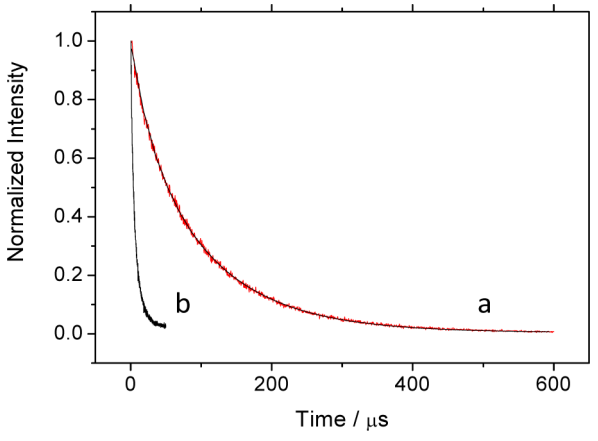

Figure 4. Representative time-resolved phosphorescence signals from PD1 recorded at 700 nm. (a) Data recorded at 21.2 °C from an air-saturated D_2O-based phosphate buffer solution. The biexponential function used to fit the data is shown. (b) Data recorded at 55.7 °C from an oxygen-saturated D_2O-based buffer solution.

(Figure 4). Rather, the data were adequately fit using a sum of two exponential functions (i.e., $A_1 \exp(-k_{T1}t) + A_2 \exp(-k_{T2}t)$). This behavior is characteristic of, and expected for, triplet states housed in a distribution of different sites, each of which is not equally accessible to quenching by $O_2(X^3\Sigma_g^-)$.[40] For the present case of PD1, it is likely that different dendrimer conformations influence oxygen diffusion in different ways and, as such, the T_1 state in one PD1 molecule is quenched by $O_2(X^3\Sigma_g^-)$ at a different rate than the T_1 state in another PD1 molecule.[22,41] (Note that biexponential decay kinetics do not necessarily mean that there are only two distinct populations of T_1 states. In this case, it only reflects one way to quantify a distribution of T_1 states characterized by a distribution of dendrimer conformations.) This increase in the complexity of T_1 decay is readily accommodated in the expression shown in Figure 3 through which we determine the $O_2(a^1\Delta_g)$ lifetime; we simply substitute the sum of two exponential functions (i.e., $A_1 \exp(-k_{T1}t) + A_2 \exp(-k_{T2}t)$) for the single exponential term (i.e., $\exp(-k_Tt)$). [Although we initially enter a sum of exponentials to represent T_1 decay, our iterative fitting routine converges on values of A_1 and A_2 that have a different sign. This is expected given that the value of k_Δ is bracketed by k_{T1} and k_{T2}.] Averaged results of the biexponential fits to the decay of PD1 phosphorescence are shown in Table 1.

We performed the following control experiment to further aid our interpretation of the time-resolved $O_2(a^1\Delta_g)$ phosphorescence decay traces. We replaced the band-pass interference filter (fwhm = 50 nm) used to spectrally isolate the 1275 nm phosphorescence of $O_2(a^1\Delta_g)$ with a 1200 nm band-pass interference filter (fwhm = 20 nm). At this latter wavelength, $O_2(a^1\Delta_g)$ does not emit.[42,43] Nevertheless, we were able to record an emission signal, which based on the decay kinetics, clearly originates from the T_1 state of PD1. These data indicate that the PD1 emission spectrum extends out into the near IR, and depending on the experiment, ~10–15% of the signal detected at 1275 nm does not originate from $O_2(a^1\Delta_g)$ at all but is emission from the PD1 T_1 state. This point was substantiated in a separate control experiment in which we removed all of the $O_2(a^1\Delta_g)$ phosphorescence at 1275 nm by the addition of a $O_2(a^1\Delta_g)$ quencher (vide infra). Under these latter conditions, the residual emission signal at 1275 nm was likewise assigned to PD1 phosphorescence based on the decay kinetics (Figure 3), which corresponded to those independently observed at 700 and 1200 nm. The PD1 emission data thus obtained were subtracted from all 1275 nm data prior to the application of our fitting routine to obtain k_Δ.

Independent experiments were also performed at a given temperature and oxygen concentration where bovine serum albumin, BSA, was added to the PD1 solution. BSA is an efficient quencher of $O_2(a^1\Delta_g)$ with $k_q = 5 \times 10^8$ s^{-1} M^{-1}, and as a large protein, it does not penetrate certain enclosures (e.g., plasma membrane of certain cells).[18,44] On this basis, the expectation is that BSA will not penetrate the dendrimer enclosure, and this is consistent with the fact that it does not affect the T_1 decay of PD1.[22] As such, BSA will only quench the PD1-sensitized $O_2(a^1\Delta_g)$ that escapes into the bulk solvent. Values of k_Δ obtained when BSA was added over the concentration range 2–4 mM indicate that, within the limits of our measurements, all of the $O_2(a^1\Delta_g)$ produced by the Pd porphyrin escapes into the bulk medium [i.e., with 2 mM BSA, τ_Δ was reduced to ~1 μs, as expected given $k_q = 5 \times 10^8$ s^{-1} M^{-1}, and this is consistent with BSA quenching >98.5% of the $O_2(a^1\Delta_g)$ produced]. An example of the data recorded is shown in Figure 3.

PD1 Is a Poor $O_2(a^1\Delta_g)$ Quencher. Our data indicate that PD1 is a poor $O_2(a^1\Delta_g)$ quencher, even at the comparatively high concentration (100 μM) used in our two-photon experiments. Specifically, when PD1 is dissolved in D_2O at a

dx.doi.org/10.1021/jp304954m | J. Phys. Chem. B 2012, 116, 10234–10246

concentration of 100 μM, we are unable to discern a change in τ_Δ compared to the value expected for neat D_2O (i.e., $\tau_\Delta \approx 68$ μs at 21 °C[45]). This observation was confirmed by independently producing $O_2(a^1\Delta_g)$ upon irradiation of a different sensitizer (methylene blue) in a solution that also contained 100 μM PD1. The point here is that, although porphyrins that are not encased generally remove $O_2(a^1\Delta_g)$ with the comparatively large bimolecular rate constant of $\sim 10^7-10^9$ s^{-1} M^{-1},[46] the dendrimer enclosure itself is a poor $O_2(a^1\Delta_g)$ quencher and effectively shields the porphyrin from $O_2(a^1\Delta_g)$. As a result, the bimolecular porphyrin-mediated quenching process cannot kinetically compete with the pseudo first-order solvent-mediated deactivation of $O_2(a^1\Delta_g)$.

Fraction of Triplet States Quenched by $O_2(X^3\Sigma_g^-)$. Under conditions where T_1 deactivation follows first-order kinetics, the fraction of T_1 states quenched by $O_2(X^3\Sigma_g^-)$, f_T, is readily obtained by quantifying the T_1 decay rate, k_T, under nitrogen as well as air (or oxygen) saturated conditions (eq 2).

$$f_T = 1 - \frac{k_T^{N2}}{k_T^{air}} \tag{2}$$

This approach is readily extended to the case where T_1 decay is expressed as a sum of two exponential functions; one simply normalizes the respective terms by the expansion coefficients, A_1 and A_2, obtained from the biexponential fit (eq 3). The data thus obtained from our PD1 phosphorescence measurements are likewise presented in Table 1.

$$f_T = \frac{A_1}{A_1 + A_2}\left(1 - \frac{k_{T1}^{N2}}{k_{T1}^{air}}\right) + \frac{A_2}{A_1 + A_2}\left(1 - \frac{k_{T2}^{N2}}{k_{T2}^{air}}\right) \tag{3}$$

Summarizing the Oxygen-Related Behavior of PD1. For data recorded in D_2O-based buffer solutions upon the irradiation of PD1, we reach the following conclusions: (1) The $O_2(a^1\Delta_g)$ lifetime, $\tau_\Delta = 1/k_\Delta$, decreases with an increase in temperature, and the values obtained under the conditions in which ϕ_Δ for PD1 was recorded are consistent with those independently recorded for a population of $O_2(a^1\Delta_g)$ in bulk D_2O.[45] (2) The fraction of the PD1 triplet state quenched by oxygen, f_T, as determined using eq 3, increases with an increase in both temperature and oxygen concentration, as expected. (3) At all temperatures and oxygen concentrations examined, the PD1-sensitized $O_2(a^1\Delta_g)$ quantum yield is equivalent to f_T. Thus, the interaction between the T_1 state of PD1 and $O_2(X^3\Sigma_g^-)$ produces $O_2(a^1\Delta_g)$ with unit efficiency (i.e., $S_\Delta \approx 1.0$). (4) The fact that $\phi_\Delta \approx f_T$ likewise indicates that $\phi_T \approx 1.0$, which is expected for such a Pd porphyrin.[47] The pertinent data are summarized in Table 1.

Two-Photon Absorption Cross-Sections. To quantify the $O_2(a^1\Delta_g)$ dose in a photosensitized experiment, it is necessary to quantify the probability of light absorption by the sensitizer. For two-photon excitation of the sensitizer, this means quantifying the two-photon absorption cross-section, $\delta(\lambda)$, preferably at a variety of wavelengths λ that might be used in different experiments.

Experiments performed to this end involved comparing the probability of a two-photon initiated process in PD1 to the probability of a two-photon initiated process in a standard molecule for which $\delta(\lambda)$ is known. Specifically, the intensity of two-photon initiated PD1 phosphorescence was compared to the intensity of $O_2(a^1\Delta_g)$ phosphorescence sensitized upon two-photon excitation of the reference standard. These particular experiments were chosen because the decay kinetics and wavelengths of the emitted light that is monitored are similar, and thus, only minor changes needed to be made in the respective experiments (i.e., simple filter changes). Moreover, we opted to use PD1 phosphorescence and not PD1-sensitized $O_2(a^1\Delta_g)$ phosphorescence to avoid the extra complication of working with the $O_2(a^1\Delta_g)$ kinetics discussed in the previous section. In all cases, a log–log plot of the intensity of the given emission signal against the incident laser power had a slope of 2.0 ± 0.1, as expected for a two-photon process.

Using a femtosecond-laser-based approach outlined in previous publications[26,27,48] and 2,5-dibromo-1,4-bis(2-(4-diphenyl-aminophenyl)vinyl)-benzene as the reference standard,[26,27] values of δ for PD1 were obtained at four different wavelengths (Table 2). The wavelengths chosen for the two-photon measurements cover a range that is conveniently accessible from common femtosecond laser systems. The absorption cross-sections obtained are consistent with what is expected for porphyrins and metalloporphyrins.[49,50]

Table 2. Two-Photon Absorption Cross-Sections, δ, for PD1 in D_2O

λ (nm)	λ(fwhm)[a] (nm)	δ (GM)[b]
783	12	33.3 ± 5.0
800	12	27.9 ± 4.2
820	14	18.9 ± 2.8
832	13	16.7 ± 2.5

[a]Spectral distribution at the given wavelength.[26] [b]1 GM = 10^{-50} cm^4 s $photon^{-1}$ $molecule^{-1}$.

Singlet-Oxygen-Mediated Cell Death. *Establishing Distance-Dependent Parameters.* A key aspect of the foundation upon which this study is built is that $O_2(a^1\Delta_g)$ has a prescribed sphere of activity that reflects its diffusion away from its point of production over a finite period defined by its lifetime.[2] In the extracellular medium used for our experiments, the $O_2(a^1\Delta_g)$ lifetime is determined not just by the solvent (either H_2O or D_2O) but also by the presence of solutes (e.g., added nutrients, buffers) that act as quenchers. In this regard, we have independently established that PD1 itself is a poor $O_2(a^1\Delta_g)$ quencher, even at the comparatively high concentration (100 μM) used in our two-photon experiments (vide supra).

As presented in subsequent sections, cell kill experiments were performed using different extracellular media. In one set of experiments, PD1 was dissolved in a growth medium, which contained, in particular, dissolved amino acids and vitamins, some of which are efficient $O_2(a^1\Delta_g)$ quenchers/reactants. In other experiments, we used our so-called Standard Maintenance Medium (SMM) which lacks the amino acids. To quantify the pertinent distance-dependent spheres of activity for $O_2(a^1\Delta_g)$, it is necessary to quantify the $O_2(a^1\Delta_g)$ lifetime in these respective media. This was done in independent cuvette-based experiments. In light of the complexity associated with determining τ_Δ in a PD1-sensitized experiment (vide supra), we opted to measure these lifetimes using an independent $O_2(a^1\Delta_g)$ sensitizer that absorbs light at a much longer wavelength than does the PD1 also present in solution. To this end, methylene blue was added to the solution and irradiated at 610 nm. The $O_2(a^1\Delta_g)$ phosphorescence signals thus obtained followed first-order decay kinetics, as expected,

dx.doi.org/10.1021/jp304954m | J. Phys. Chem. B 2012, 116, 10234–10246

and τ_Δ values were readily obtained from single exponential fits to the data.

In the D_2O-based version of the growth medium, the $O_2(a^1\Delta_g)$ lifetime ($\tau_\Delta = 39 \pm 2$ μs) is determined principally by the added amino acids. In the corresponding H_2O-based version of the growth medium, where solvent exerts a greater effect on inducing the $O_2(a^1\Delta_g) \rightarrow O_2(X^3\Sigma_g^-)$ transition, the $O_2(a^1\Delta_g)$ lifetime is 3.1 ± 0.1 μs. To complement previously published work, we opt to use a HEPES buffer in our SMM instead of the bicarbonate buffer used in the growth medium.[25] Although HEPES does not react with $O_2(a^1\Delta_g)$, as is the case with selected amino acids, it is nevertheless a $O_2(a^1\Delta_g)$ quencher that promotes the $O_2(a^1\Delta_g) \rightarrow O_2(X^3\Sigma_g^-)$ transition.[25] In the D_2O-based version of SMM, the $O_2(a^1\Delta_g)$ lifetime is 41 ± 2 μs, whereas the lifetime is 3.1 ± 0.1 μs in the corresponding H_2O-based solution. These lifetime data are summarized in Table 3.

Table 3. $O_2(a^1\Delta_g)$ Lifetimes and Estimated Root-Mean-Square Diffusion Distances in Selected Media

solution	$\tau_\Delta{}^a$ (μs)	d(radial)^b (nm)
neat H_2O	3.5 ± 0.1	355
neat D_2O	68 ± 1	1565
H_2O growth medium w/ 100 μM PD1	3.1 ± 0.1	334
D_2O growth medium w/ 100 μM PD1	39 ± 2	1185
H_2O maintenance medium w/ 100 μM PD1	3.1 ± 0.1	334
D_2O maintenance medium w/ 100 μM PD1	41 ± 2	1215

[a]Determined using methylene blue as the sensitizer. See discussion in the text. [b]Calculated using the expression for radial diffusion, $d = (6tD)^{1/2}$, and a time period, t, of three $O_2(a^1\Delta_g)$ lifetimes.

We can estimate the root-mean-square distance d that $O_2(a^1\Delta_g)$ would move in a time period t using the following expression for radial diffusion (eq 4):[51,52]

$$d = \sqrt{6tD} \tag{4}$$

where D is the diffusion coefficient for oxygen in that given medium. This expression quantifies the spread of $O_2(a^1\Delta_g)$ molecules after time t under conditions in which they can move in all directions (i.e., forward and backward). In this estimate, we assume that the value of D for oxygen in water (2×10^{-5} cm^2 s^{-1})[53] is valid.[54] We likewise assume that it is appropriate to consider a time period t equivalent to 3× the $O_2(a^1\Delta_g)$ lifetime in that given medium (i.e., after three lifetimes, 5% of the $O_2(a^1\Delta_g)$ originally produced by the pulsed laser still remains in solution). The values of d obtained using eq 4 that correspond to the $O_2(a^1\Delta_g)$ lifetimes under our experimental conditions are likewise shown in Table 3.

With these $O_2(a^1\Delta_g)$ diffusion distances in mind, we now consider how far away from the edge of a cell one should try to produce $O_2(a^1\Delta_g)$ in order to facilitate appreciable interaction between $O_2(a^1\Delta_g)$ and the cell. The pertinent parameters are illustrated in Figure 5. A collimated beam of light passed through a lens (e.g., our microscope objective) will produce the so-called Airy intensity distribution at the focus.[55] In the plane orthogonal to the axis of light propagation, the distance from the maximum to the first minimum of this distribution, r_0, is given by

$$r_0 = \frac{0.61\lambda}{NA} \tag{5}$$

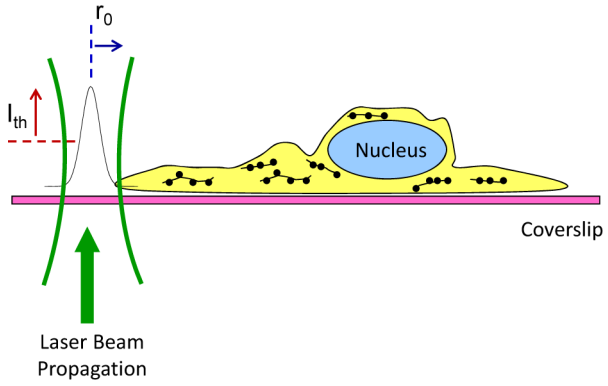

Figure 5. Cartoon illustrating selected parameters that influence the two-photon excitation of an extracellular $O_2(a^1\Delta_g)$ sensitizer. The coverslip lies in the $x-y$ plane, which is orthogonal to the axis of laser beam propagation (z axis). The core of the Airy intensity distribution at the waist of the focused laser beam in the $x-y$ plane is shown as a black line. The distance from the maximum to the first minimum of the Airy profile is denoted r_0, and the intensity threshold required for two-photon excitation is shown as I_{th}.

where λ is the wavelength of light used, and NA is the numerical aperture of the lens.[12,55] With the optics used to focus our 820 nm excitation light onto the microscope coverslip, we expect a diffraction-limited radius r_0 at the focused beam waist of ~550 nm (i.e., incident light will extend out laterally for about 550 nm from the center of the focus).[11] However, given that an intensity threshold, I_{th}, must first be achieved before two-photon excitation can be realized, the pertinent distance from the center of the focus in which excited states are created will be $<r_0$, certainly with low incident laser powers.

For focused light along the axis of propagation, one can write a similar expression for the distance, z_0, between the maximum and first minimum of the intensity distribution:[12]

$$z_0 = \frac{2n\lambda}{(NA)^2} \tag{6}$$

where n is the refractive index of the medium between the microscope objective and the sample (water in our case). Under our conditions, $z_0 \approx 2.7$ μm and is approximately equivalent to the thickness of a cell on a coverslip.

On the basis of these simplistic arguments and the data shown in Table 3, it is expected that, if the center of our focused laser beam is placed ~1 μm away from the edge of the cell, a sufficient amount of $O_2(a^1\Delta_g)$ produced in a D_2O-based medium should reach the cell, whereas little of the $O_2(a^1\Delta_g)$ produced in an H_2O-based medium will reach the cell. If the center of the focused laser beam is placed ~2 μm away from the cell edge, very little of the $O_2(a^1\Delta_g)$ produced in the D_2O-based medium will reach the cell. Although we elaborate further on these geometry issues in a separate section below, these estimates are sufficient to establish proof-of-principle in cell death experiments.

Assessing Cell Death: The Tools. In an earlier study, we ascertained that $O_2(a^1\Delta_g)$ produced upon one-photon excitation of an extracellular sensitizer could kill HeLa cells.[20] For the present study, with our desire to establish a better-controlled spatially localized source of $O_2(a^1\Delta_g)$, it is necessary to define the conditions under which focused two-photon excitation of PD1 influences cell viability.

dx.doi.org/10.1021/jp304954m | J. Phys. Chem. B 2012, 116, 10234−10246

Two approaches were used to assess cell response to two-photon irradiation of PD1: (1) Bright field images were used to record morphology changes associated with cell death (e.g., membrane located vacuole formation, chromatin condensation, and cell shrinkage). This is an established method that combines reasonable accuracy with ease of implementation.[10,17,18,20,56,57] (2) The assay based on the Alexa Fluor 680 Annexin V conjugate was used.[58] The Annexin V assay is often described as a test for the externalization of phosphatidylserine on the plasma membrane to which the Annexin V protein binds; a process that can be an indicator of early/intermediate stages of apoptotic death.[59,60] However, it is important to note several caveats. First, Annexin V can also bind to phosphatidylserine in necrotic death as a consequence of the general disruption of the integrity of the plasma membrane.[59,61] Thus, caution should be exercised in assigning a positive Annexin response solely to apoptotic death. Second, Annexin V will also bind to products of lipid peroxidation on the membrane (e.g., aldehydes),[62] not just to phosphatidylserine. As a consequence, there may be cases where a positive Annexin V response may not correlate with cell death at all. This latter caveat is certainly pertinent given the oxygenation experiments performed in this study, and we return to this point in our discussion below.

Assessing Cell Death: Experiments in the Growth Medium. For controlled $O_2(a^1\Delta_g)$-mediated cell death using an extracellular sensitizer, the first variable that must be regulated is the medium surrounding the cell. A good starting point is to consider the medium that is arguably expected to adversely affect the cells the least: a growth or culturing medium. In this case, however, we ascertained that the nutrients (i.e., amino acids) characteristically present in the growth medium cause a problem. Specifically, data obtained are consistent with a process in which the PD1-sensitized $O_2(a^1\Delta_g)$ oxygenates/oxidizes the dissolved amino acids. This is most simply illustrated by pointing to the $O_2(a^1\Delta_g)$ lifetime of 39 μs in the D_2O-based growth medium (Table 3), which reflects $O_2(a^1\Delta_g)$ removal channels dominated by reaction with selected amino acids (e.g., tryptophan, tyrosine, and histidine). The products of these oxygenation reactions (e.g., hydroperoxides)[63,64] are comparatively long-lived and can diffuse over greater distances than $O_2(a^1\Delta_g)$. Most importantly, these peroxides can likewise adversely influence the cell in ways that may result in cell death.[63,64] These latter points were confirmed in an independent experiment in which we first photosensitized the production of $O_2(a^1\Delta_g)$ using PD1 in a solution of our growth medium. Immediately thereafter, and in the absence of light, we then added this solution containing photooxygenated amino acids to a cell culture. As expected, the cells died due, presumably, to the long-lived peroxides present in the medium that had been irradiated.

It is reasonable to expect that the mechanism(s) of cell death initiated by such peroxides will be different from those initiated by direct interaction of $O_2(a^1\Delta_g)$ with the cell, and as a consequence, the cell response(s) may likewise be different. One way in which this point can be examined is to monitor cell response in H_2O- and D_2O-based growth media, exploiting the fact that $O_2(a^1\Delta_g)$ has a different lifetime and diffusion distance in these solvents (Table 3), whereas peroxide diffusion should be independent of the solvent. Although differences in cell response are indeed observed for experiments performed under these conditions (Figures 6 and 7), care must be exercised not to overinterpret the data; as with all the cell experiments in this

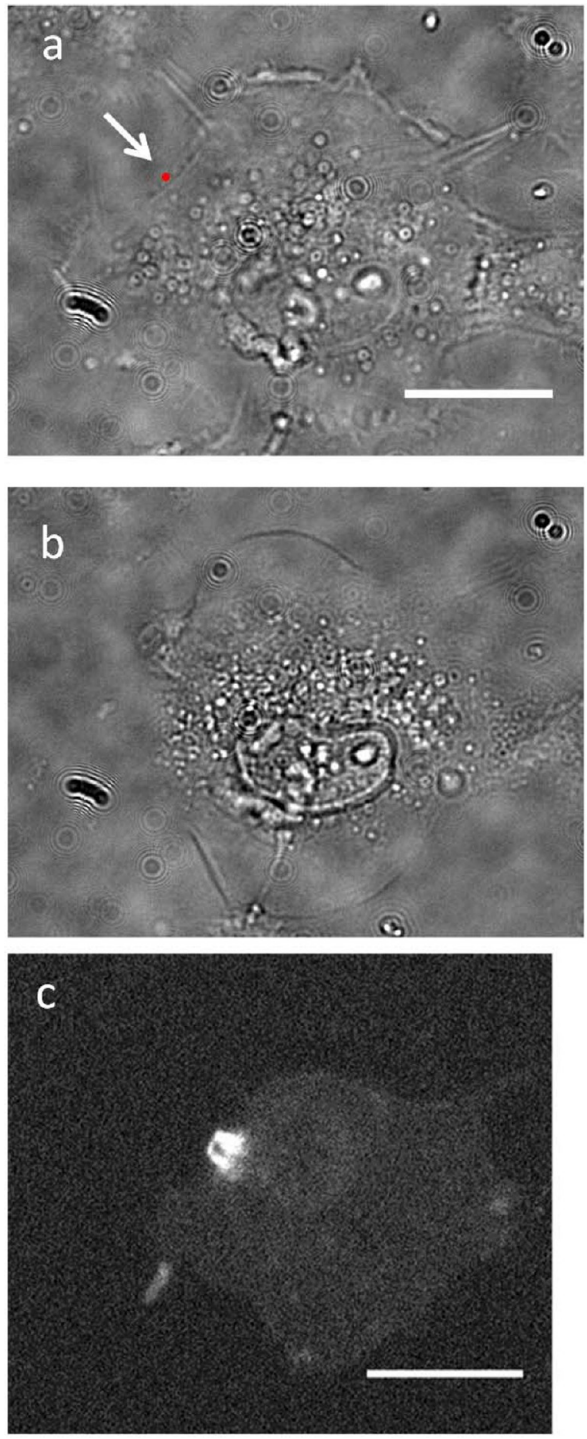

Figure 6. Effect of 820 nm irradiation of PD1 on a HeLa cell in D_2O-based growth medium. (a) Bright field image of the sample before irradiation. The red dot (arrow) indicates the position of the focused irradiation ~1 μm away from the cell edge. Scale bar = 20 μm. (b) Bright field image taken after 25 min of irradiation with 6.6 mW at the sample. Morphological signs indicative of cell death are clearly visible. (c) Fluorescence image of the cell based on the Annexin conjugate, likewise recorded after 25 min of irradiation. The site on the cell immediately adjacent to the site of irradiation clearly gives a more pronounced Annexin response. As explained in the text, these data likely represent cell response to a combination of $O_2(a^1\Delta_g)$ and peroxides formed as a consequence of the $O_2(a^1\Delta_g)$-mediated oxygenation of amino acids in the medium.

dx.doi.org/10.1021/jp304954m | J. Phys. Chem. B 2012, 116, 10234−10246

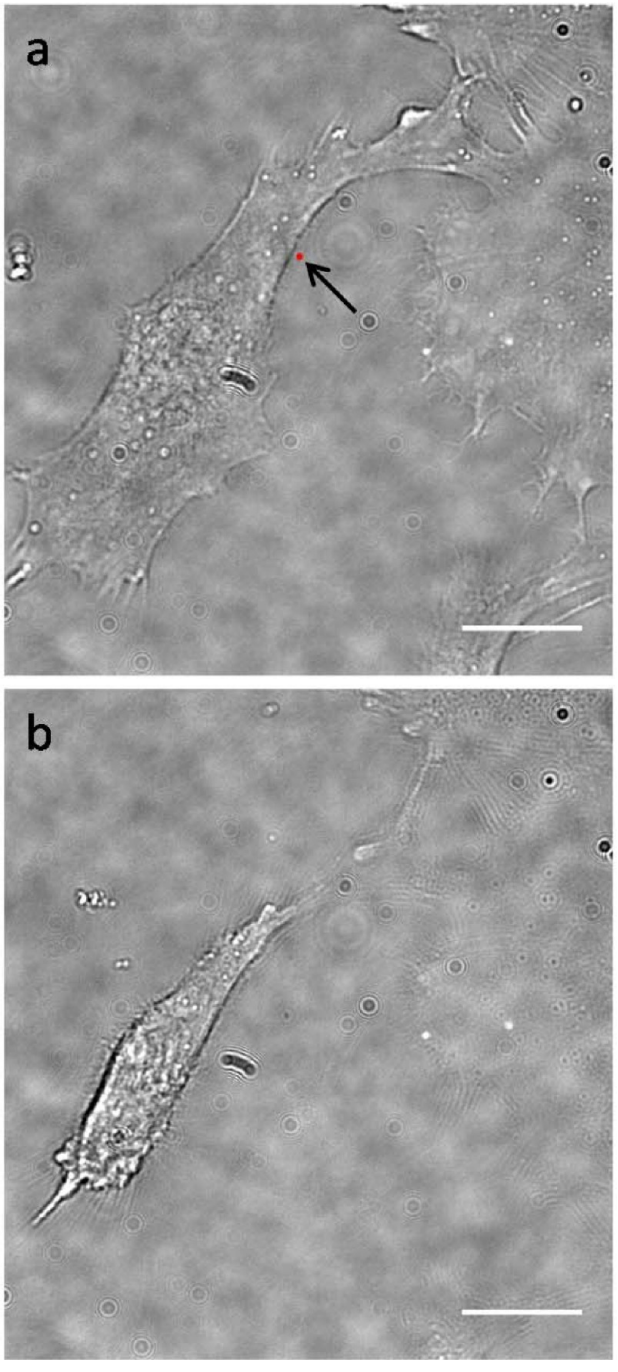

Figure 7. Effect of 820 nm irradiation of PD1 on a HeLa cell in H_2O-based growth medium. (a) Bright field image of the sample before irradiation. The red dot (arrow) indicates the position of the focused irradiation ~1 μm away from the cell edge. (b) Bright field image taken after 45 min of irradiation with 6.6 mW at the sample. Although the clear shrinking of the cell is characteristic of death, a positive Annexin stain was not observed, even 2 h after irradiation ceased. These data likewise represent cell response to both $O_2(a^1\Delta_g)$ and to peroxides formed as a consequence of the $O_2(a^1\Delta_g)$-mediated oxygenation of amino acids in the medium, albeit in different proportions to that shown in Figure 6. Scale bar = 20 μm.

proof-of-principle report, a statistically significant population of cells has yet to be examined.

In conclusion, from the perspective of elucidating mechanism(s) of cell death mediated by extracellular $O_2(a^1\Delta_g)$, the use of a growth medium containing amino acids is likely to be more of a hindrance than an asset.

Assessing Cell Death: Experiments in the Maintenance Medium. To ensure that $O_2(a^1\Delta_g)$ is the only extracellular reactive intermediate initiating cell death upon PD1 irradiation, experiments were performed using our so-called Standard Maintenance Medium (SMM) that, among other things, lacks solutes that can be oxidized by $O_2(a^1\Delta_g)$. In independent experiments, we ascertained that, in the absence of light absorption by a $O_2(a^1\Delta_g)$ sensitizer, HeLa cells remain viable in our D_2O-based SMM for at least 2−3 h and ~3−5 h in our H_2O-based SMM.[18,25] As outlined below, these periods of time are sufficiently long to ensure accurate measures of photo-induced $O_2(a^1\Delta_g)$-mediated death.

For these proof-of-principle studies, we are able to demonstrate three general kinds of cell response depending on the $O_2(a^1\Delta_g)$ dose to which the cell was exposed. First, and as expected, we did not observe an adverse response from a cell under conditions in which the $O_2(a^1\Delta_g)$ that was produced could not reach the cell (i.e., diffusion distance was too large, Table 3). Second, cells that were exposed to a moderate dose of $O_2(a^1\Delta_g)$ appeared to be able to combat and repair the effects of this insult. Third, cells exposed to a large $O_2(a^1\Delta_g)$ dose showed clear signs of death. Examples of the latter two categories are provided below.

For HeLa cells in D_2O-based SMM containing 100 μM PD1, irradiation for a period of ~30 min with an average power at the sample of ~10 mW with 820 nm focused to a spot whose center is ~1 μm away from the cell edge generally results in some kind of cell response within 0.5−1.0 h after irradiation is stopped. When we irradiate for a shorter period of time or use a smaller power, it is generally difficult to note any change in cell morphology over this same time period. An example of cell response to this moderate dose of $O_2(a^1\Delta_g)$ is illustrated in Figure 8. Under these conditions, the cell appears to be able to repair the $O_2(a^1\Delta_g)$-initiated damage, leaving only a "slight scar" that stains Annexin V positive. Admittedly, although this cell appears to have survived this $O_2(a^1\Delta_g)$ insult, we may, nevertheless, have made it more susceptible to death at a later time. The latter is a point that needs to be investigated further.

In Figure 9, we show the results of cell exposure to a large dose of $O_2(a^1\Delta_g)$. Vacuole formation characteristic of death is visible in the bright field image, and the cell stains Annexin V positive. As in Figure 6, the site on the cell immediately adjacent to the site of irradiation and $O_2(a^1\Delta_g)$ production gives a more pronounced Annexin response. We infer that membrane damage here must be quite extensive, as reflected in either a greater amount of externalized phosphatidylserine or products of lipid peroxidation.

These observations of a different local response to $O_2(a^1\Delta_g)$ also need to be considered in light of the cell topography and contents immediately adjacent to the site of $O_2(a^1\Delta_g)$ production. Of course, one must first consider the morphology and content of the membrane itself. If $O_2(a^1\Delta_g)$ encounters a domain characterized, for example, by many lipid rafts that contain higher concentrations of proteins and cholesterol,[65] it is likely that the initial adverse effects of $O_2(a^1\Delta_g)$ will be localized at that point on the membrane. However, in domains where membrane proteins are sparse, it is likely that $O_2(a^1\Delta_g)$ will propagate further into the cytoplasm and possibly initiate different events at a specific organelle.

In control experiments, we established that $O_2(a^1\Delta_g)$ is indeed the pertinent reactive intermediate responsible for

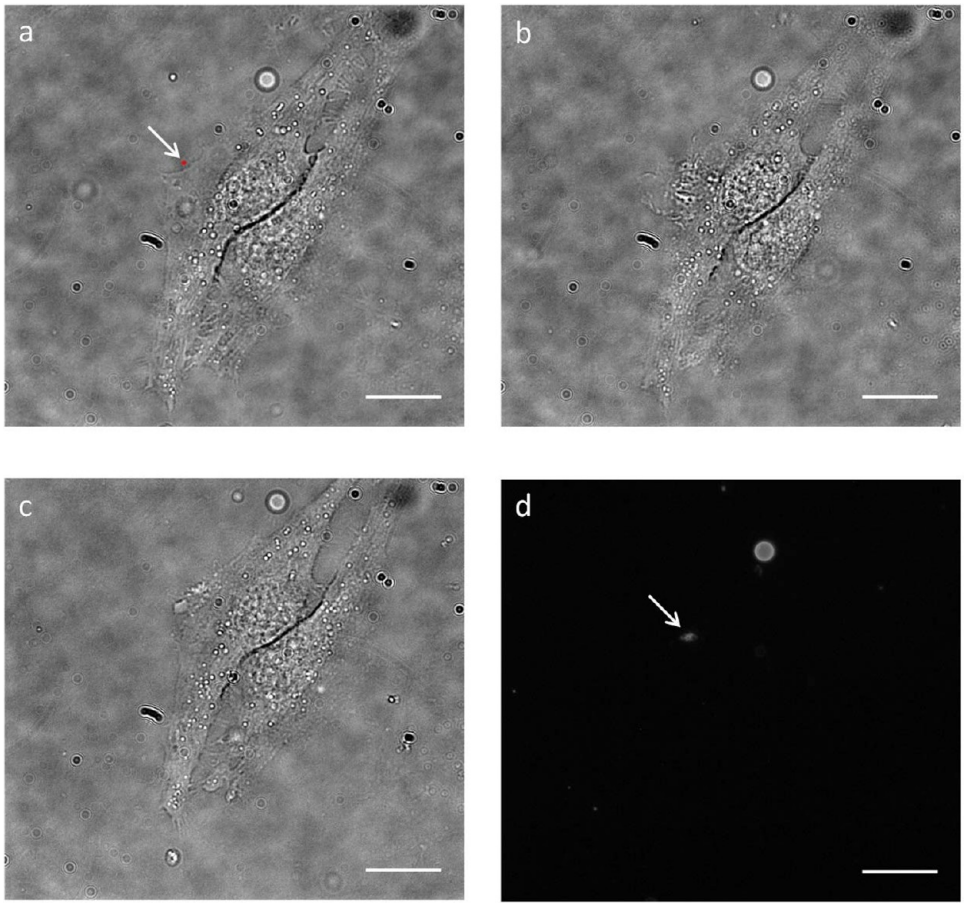

Figure 8. Effect of 820 nm irradiation of PD1 on a HeLa cell in the D_2O-based standard maintenance medium, SMM. (a) Bright field image of the sample before irradiation. The red dot (arrow) indicates the position of the focused irradiation ~1 μm away from the cell edge. (b) Bright field image taken after 30 min of irradiation with 13 mW at the sample. Damage on the cell adjacent to the site of irradiation is clearly visible. (c) Bright field image taken 1 h after the irradiation was ceased. Evidence of cell death is not visible. Rather, the cell appears to have repaired the damage. (d) Fluorescence image of the cell based on the Annexin V conjugate, likewise recorded 1 h after irradiation ceased. Only the repaired spot gives a positive Annexin response (arrow). Scale bar = 20 μm.

adverse cell response in these studies. Specifically, upon the addition of an efficient $O_2(a^1\Delta_g)$ quencher to the D_2O-based SMM (10 mM NaN_3), we were unable to perturb the cells upon irradiation of PD1. [Although NaN_3 is itself cytotoxic over long time periods, it is benign over the time periods of our studies.[20,66]]

In independent experiments, we also observed that, under conditions of a long irradiation period with a high laser power at a point near the cell membrane, we can affect the cell through the process of optoporation (i.e., local plasma formation that produces a shock wave that can perturb the cell membrane).[67,68] However, the bright field and annexin-based images indicate that we do not kill the cell via optoporation (e.g., we might record an annexin image similar to that shown in Figure 8d). In our complementary one-photon extracellular experiments,[20] optoporation was not a problem, in part, because the irradiation periods and laser powers were much smaller. In any event, for the present experiments, it was desirable to work with a D_2O-based medium, which allowed us to position the focused laser further away from the cell membrane and thus mitigate the effects of optoporation.

Quantifying Pertinent Parameters for Dosimetry. On the basis of material we have presented thus far, it should be apparent that we can readily perform photoinitiated $O_2(a^1\Delta_g)$-mediated cell death experiments in which the amount and location of the $O_2(a^1\Delta_g)$ produced is regulated. In itself, this is already a significant advance. However, a measure of the amount of $O_2(a^1\Delta_g)$ that encounters the cell requires more information, and the uncertainties on the parameters relevant here currently make an absolute assessment of an effective $O_2(a^1\Delta_g)$ dose challenging. Nevertheless, it is prudent to briefly estimate the amount of $O_2(a^1\Delta_g)$ produced in these proof-of-principle experiments and to discuss pertinent limiting issues.

Amount and Concentration of $O_2(a^1\Delta_g)$ Produced. Features of our experimental approach over which we have control or that we have quantified are (1) the PD1 concentration, (2) the PD1 two-photon absorption cross-section, (3) the PD1-sensitized quantum yield of $O_2(a^1\Delta_g)$ production, (4) the laser power incident on the sample, and (5) the microscope optics used to focus the light at the sample. In the least, this means that we can calculate, with reasonable accuracy, the concentration of PD1 excited states in the homogeneous extracellular domain that is irradiated.

The pertinent expression to this end is shown in eq 7,[26] where N_2 is the number of PD1 S_1 excited states produced upon two-photon excitation at a given wavelength, λ, and concentration of PD1:

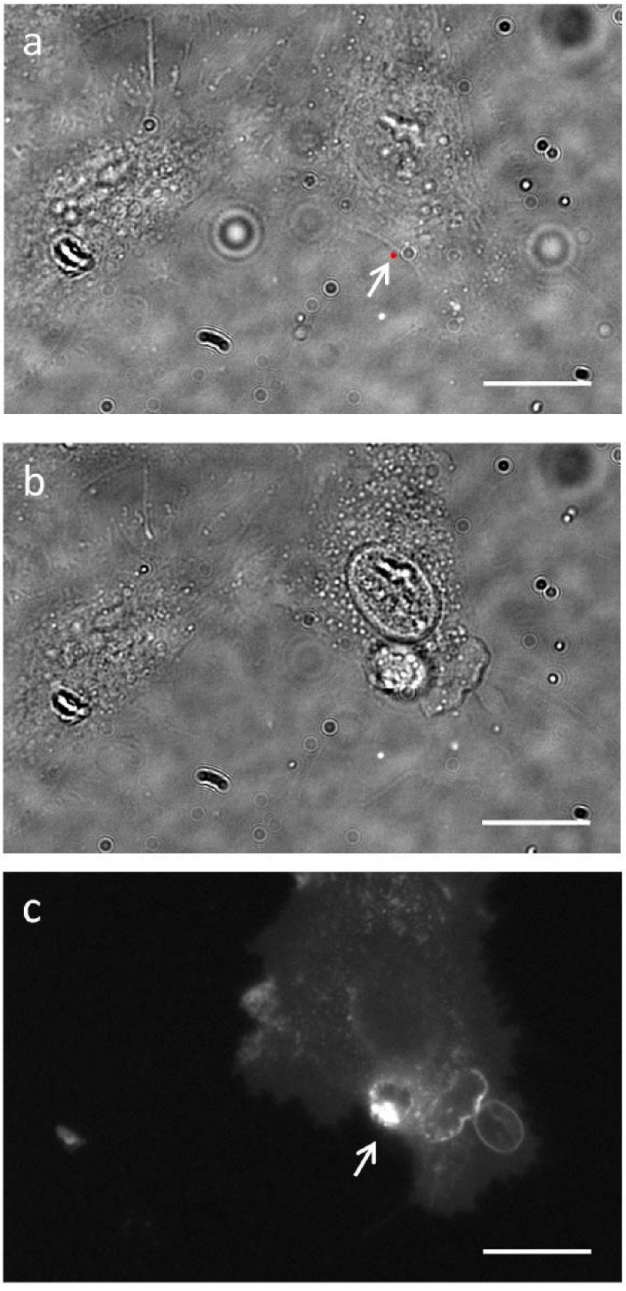

Figure 9. Effect of 820 nm irradiation of PD1 on a HeLa cell in the D_2O-based standard maintenance medium, SMM. (a) Bright field image of the sample before irradiation. The red dot (arrow) indicates the position of the focused irradiation ~1 μm away from the cell edge. (b) Bright field image taken after 45 min of irradiation with 13 mW at the sample. Morphological evidence of cell death is clearly visible. (c) Fluorescence image of the cell based on the Annexin conjugate, likewise recorded after 30 min of irradiation. Although the entire cell stains Annexin positive, the position adjacent to the site of irradiation clearly gives a unique response (arrow). Scale bar = 20 μm.

$$N_2 = \frac{\delta P_{avg}^2 \lambda^2 [PD1]}{2 f^2 c^2 h^2} g_t g_s \quad (7)$$

In addition to the average laser power, P_{avg}, and frequency, f, of the pulsed femtosecond laser used, it is necessary to quantify the temporal and spatial coherence factors, g_t and g_s, respectively. This is readily done for Gaussian beams whose temporal and spatial profiles at the given wavelength have been independently characterized.[26]

For experiments performed under our conditions with an average power of 10 mW at 820 nm, we obtain $N_2 \approx 9.7 \times 10^{-22}$ moles of PD1 S_1 produced per laser pulse. With the values of r_0 and z_0 obtained using eqs 5 and 6, and making the crude assumption that the excitation volume is a right circular cylinder, we obtain a pertinent volume of 2.4×10^{-15} L, and this yields a concentration of $\sim 4 \times 10^{-7}$ M S_1 states produced per pulse. Partial experimental quantification of the pertinent volume could be achieved, for example, by recording spatially resolved images of the PD1 phosphorescence, particularly if subdiffraction-limit imaging techniques can be employed.[69]

Carrying these results further using $\phi_\Delta \approx 0.92$, we obtain a concentration of $O_2(a^1\Delta_g)$ produced in the excitation volume of $\sim 3.7 \times 10^{-7}$ M. However, considering that $O_2(a^1\Delta_g)$ will diffuse over an appreciable distance within its lifetime (i.e., data in Table 3), the more pertinent concentration of $O_2(a^1\Delta_g)$ produced per pulse is $\sim 2.4 \times 10^{-8}$ M. Unfortunately, corresponding experimental confirmation of this latter volume using the 1275 nm $O_2(a^1\Delta_g) \rightarrow O_2(X^3\Sigma_g^-)$ phosphorescence as a probe will be difficult. The Rayleigh or diffraction limit that defines the maximum resolution with which an image can be generated at λ = 1275 nm using a lens with a numerical aperture of 0.9 is likewise about 1 μm.[70,71] This latter point, coupled with the current experimental limitations associated with imaging $O_2(a^1\Delta_g)$ phosphorescence,[38,70] make this a challenging experiment, in the least.

Finally, it is useful to estimate the total number of $O_2(a^1\Delta_g)$ molecules produced under our conditions of extracellular irradiation that result in an adverse cell response. With irradiation of PD1 at 820 nm at an average power of 13 mW for 45 min (e.g., Figure 9), we produce $\sim 2 \times 10^{14}$ molecules of $O_2(a^1\Delta_g)$. This estimate is appreciably greater than a corresponding cytotoxicity-threshold-estimate of $\sim 2 \times 10^8$ $O_2(a^1\Delta_g)$ molecules in one-photon intracellular experiments.[16] Thus, extracellular singlet oxygen produced under the conditions described herein appears to be less cytotoxic than intracellular singlet oxygen.

Effect of Cell Topography and Surface Area Exposed to $O_2(a^1\Delta_g)$. Although we can provide a reasonably accurate estimate of the spatially resolved $O_2(a^1\Delta_g)$ concentration profile produced upon two-photon excitation of extracellular PD1, a key challenge in the overall dosimetry problem will be ascertaining what fraction of this $O_2(a^1\Delta_g)$ population actually encounters the cell. As one can readily infer from the cartoon in Figure 5 and discussed with reference to the data in Figures 8 and 9, different cells will present different areas, geometries of plasma membrane, and targets to the volume of photoproduced extracellular $O_2(a^1\Delta_g)$. Thus, for an accurate assessment of the effective $O_2(a^1\Delta_g)$ dose, one must also consider the cell topography and cell constituents in the domain immediately adjacent to the site of PD1 irradiation. Although elaborate methods could be used to estimate topography (e.g., AFM),[72,73] it is likely that, from a practical perspective in a cell kill experiment, one must simply infer the pertinent cell topography from a bright field image of the cell. The latter approach could also be used during the course of PD1 irradiation to account for changes in cell morphology as a consequence of $O_2(a^1\Delta_g)$-initiated perturbation (e.g., cell shrinkage). Of course, the accessible organelles lying beneath a given section of the cell membrane will be different

dx.doi.org/10.1021/jp304954m | J. Phys. Chem. B 2012, 116, 10234−10246

depending on the spatial domain chosen for PD1 irradiation, but this now becomes a variable for more systematic studies.

CONCLUSIONS

We have demonstrated that spatially localized two-photon excitation of an extracellular sensitizer can provide a much-needed reference standard to establish the relative dose of $O_2(a^1\Delta_g)$ for mechanistic studies of photoinitiated cell death. Moreover, comparing cell response to an extracellular population of $O_2(a^1\Delta_g)$ with cell response to intracellular populations of $O_2(a^1\Delta_g)$ can provide unique insight into how selected morphological and biochemical events depend on the initial oxygenation target. On the basis of these proof-of-principle experiments, quantitative studies with the proper statistical analysis can now be undertaken to more firmly establish mechanistic points underlying $O_2(a^1\Delta_g)$-mediated cell death.

AUTHOR INFORMATION

Corresponding Author

*Tel: +45 8715 5927. Fax: +45 8619 6199. E-mail: progilby@chem.au.dk.

Notes

The authors declare no competing financial interest.

ACKNOWLEDGMENTS

This work was supported by the Danish National Research Foundation and an EU Marie Curie Training Grant (TopBio PITN-GA-2010-264362). We thank Puk Lund for help with cell culturing and Dr. S. A. Vinogradov for supervising the synthesis of PD1 performed by T.V.E.

REFERENCES

(1) Clennan, E. L.; Pace, A. *Tetrahedron* **2005**, *61*, 6665−6691.
(2) Ogilby, P. R. *Chem. Soc. Rev.* **2010**, *39*, 3181−3209.
(3) Klotz, L.-O.; Kröncke, K.-D.; Sies, H. *Photochem. Photobiol. Sci.* **2003**, *2*, 88−94.
(4) Bonnett, R. *Chemical Aspects of Photodynamic Therapy*; Gordon and Breach Science Publishers: Amsterdam, The Netherlands, 2000.
(5) Redmond, R. W.; Kochevar, I. E. *Photochem. Photobiol.* **2006**, *82*, 1178−1186.
(6) Phillips, D. *Photochem. Photobiol. Sci.* **2010**, *9*, 1589−1596.
(7) Schweitzer, C.; Schmidt, R. *Chem. Rev.* **2003**, *103*, 1685−1757.
(8) Bressler, N. M.; Bressler, S. B. *Investigative Ophthal. Vis. Sci.* **2000**, *41*, 624−628.
(9) McCall, A. S.; Kraft, S.; Edelhauser, H. F.; Kidder, G. W.; Lundquist, R. R.; Bradshaw, H. E.; Dedeic, Z.; Dionne, M. J. C.; Clement, E. M.; Conrad, G. W. *Invest. Ophthalmol. Vis. Sci.* **2010**, *51*, 129−138.
(10) Pedersen, B. W.; Breitenbach, T.; Redmond, R. W.; Ogilby, P. R. *Free Radical Res.* **2010**, *44*, 1383−1397.
(11) Skovsen, E.; Snyder, J. W.; Ogilby, P. R. *Photochem. Photobiol.* **2006**, *82*, 1187−1197.
(12) Squier, J.; Müller, M. *Rev. Sci. Instrum.* **2001**, *72*, 2855−2867.
(13) Denk, W.; Strickler, J. H.; Webb, W. W. *Science* **1990**, *248*, 73−76.
(14) Collins, H. A.; Khurana, M.; Moriyama, E. H.; Mariampillai, A.; Dahlstedt, E.; Balaz, M.; Kuimova, M. K.; Drobizhev, M.; Yang, V. X. D.; Phillips, D.; Rebane, A.; Wilson, B. C.; Anderson, H. L. *Nat. Photonics* **2008**, *2*, 420−424.
(15) Dahlstedt, E.; Collins, H. A.; Balaz, M.; Kuimova, M. K.; Khurana, M.; Wilson, B. C.; Phillips, D.; Anderson, H. L. *Org. Biomol. Chem.* **2009**, *7*, 897−904.
(16) Dysart, J. S.; Patterson, M. S. *Phys. Med. Biol.* **2005**, *50*, 2597−2616.
(17) Breitenbach, T.; Kuimova, M. K.; Gbur, P.; Hatz, S.; Schack, N. B.; Pedersen, B. W.; Lambert, J. D. C.; Poulsen, L.; Ogilby, P. R. *Photochem. Photobiol. Sci.* **2009**, *8*, 442−452.
(18) Silva, E. F. F.; Pedersen, B. W.; Breitenbach, T.; Toftegaard, R.; Kuimova, M. K.; Arnaut, L. G.; Ogilby, P. R. *J. Phys. Chem. B.* **2012**, *116*, 445−461.
(19) Kuimova, M. K.; Botchway, S. W.; Parker, A. W.; Balaz, M.; Collins, H. A.; Anderson, H. L.; Suhling, K.; Ogilby, P. R. *Nat. Chem.* **2009**, *1*, 69−73.
(20) Pedersen, B. W.; Sinks, L. E.; Breitenbach, T.; Schack, N. B.; Vinogradov, S. A.; Ogilby, P. R. *Photochem. Photobiol.* **2011**, *87*, 1077−1091.
(21) Breitenbach, T.; Ogilby, P. R.; Lambert, J. D. C. *Photochem. Photobiol. Sci.* **2010**, *9*, 1621−1633.
(22) Esipova, T. V.; Karagodov, A.; Miller, J.; Wilson, D. F.; Busch, T. M.; Vinogradov, S. A. *Anal. Chem.* **2011**, *83*, 8756−8765.
(23) Nonell, S.; Gonzalez, M.; Trull, F. R. *Afinidad* **1993**, *448*, 445−450.
(24) Frederiksen, P. K.; Jørgensen, M.; Ogilby, P. R. *J. Am. Chem. Soc.* **2001**, *123*, 1215−1221.
(25) Hatz, S.; Lambert, J. D. C.; Ogilby, P. R. *Photochem. Photobiol. Sci.* **2007**, *6*, 1106−1116.
(26) Arnbjerg, J.; Johnsen, M.; Frederiksen, P. K.; Braslavsky, S. E.; Ogilby, P. R. *J. Phys. Chem. A* **2006**, *110*, 7375−7385.
(27) Arnbjerg, J.; Paterson, M. J.; Nielsen, C. B.; Jørgensen, M.; Christiansen, O.; Ogilby, P. R. *J. Phys. Chem. A* **2007**, *111*, 5756−5767.
(28) Scurlock, R. D.; Mártire, D. O.; Ogilby, P. R.; Taylor, V. L.; Clough, R. L. *Macromolecules* **1994**, *27*, 4787−4794.
(29) Marti, C.; Jürgens, O.; Cuenca, O.; Casals, M.; Nonell, S. *J. Photochem. Photobiol., A* **1996**, *97*, 11−18.
(30) Magde, D.; Wong, R.; Seybold, P. G. *Photochem. Photobiol.* **2002**, *75*, 327−334.
(31) Fleming, G. R.; Knight, A. W. E.; Morris, J. M.; Morrison, R. J. S.; Robinson, G. W. *J. Am. Chem. Soc.* **1977**, *99*, 4306−4311.
(32) Ceroni, P.; Lebedev, A. Y.; Marchi, E.; Yuan, M.; Esipova, T. V.; Bergamini, G.; Wilson, D. F.; Busch, T. M.; Vinogradov, S. A. *Photochem. Photobiol. Sci.* **2011**, *10*, 1056−1065.
(33) Lebedev, A. Y.; Cheprakov, A. V.; Sakadzic, S.; Boas, D. A.; Wilson, D. F.; Vinogradov, S. A. *ACS Appl. Mater. Interfaces* **2009**, *1*, 1292−1304.
(34) Johnsen, M.; Ogilby, P. R. *J. Phys. Chem. A* **2008**, *112*, 7831−7839.
(35) Jensen, P.-G.; Arnbjerg, J.; Tolbod, L. P.; Toftegaard, R.; Ogilby, P. R. *J. Phys. Chem. A* **2009**, *113*, 9965−9973.
(36) McGarvey, D. J.; Szekeres, P. G.; Wilkinson, F. *Chem. Phys. Lett.* **1992**, *199*, 314−319.
(37) Scurlock, R. D.; Nonell, S.; Braslavsky, S. E.; Ogilby, P. R. *J. Phys. Chem.* **1995**, *99*, 3521−3526.
(38) Snyder, J. W.; Skovsen, E.; Lambert, J. D. C.; Poulsen, L.; Ogilby, P. R. *Phys. Chem. Chem. Phys.* **2006**, *8*, 4280−4293.
(39) Ogilby, P. R.; Foote, C. S. *J. Am. Chem. Soc.* **1983**, *105*, 3423−3430.
(40) Clough, R. L.; Dillon, M. P.; Iu, K.-K.; Ogilby, P. R. *Macromolecules* **1989**, *22*, 3620−3628.
(41) Rozhkov, V.; Wilson, D.; Vinogradov, S. A. *Macromolecules* **2002**, *35*, 1991−1993.
(42) Macpherson, A. N.; Truscott, T. G.; Turner, P. H. *J. Chem. Soc., Faraday Trans.* **1994**, *90*, 1065−1072.
(43) Wessels, J. M.; Rodgers, M. A. J. *J. Phys. Chem.* **1995**, *99*, 17586−17592.
(44) Skovsen, E.; Snyder, J. W.; Lambert, J. D. C.; Ogilby, P. R. *J. Phys. Chem. B* **2005**, *109*, 8570−8573.
(45) Jensen, R. L.; Arnbjerg, J.; Ogilby, P. R. *J. Am. Chem. Soc.* **2010**, *132*, 8098−8105.
(46) Wilkinson, F.; Helman, W. P.; Ross, A. B. *J. Phys. Chem. Ref. Data* **1995**, *24*, 663−1021.
(47) Gouterman, M. In *The Porphyrins*; Dolphin, D., Ed.; Academic Press: New York, 1978; Vol. 3, pp 1−165.

(48) Johnsen, M.; Paterson, M. J.; Arnbjerg, J.; Christiansen, O.; Nielsen, C. B.; Jørgensen, M.; Ogilby, P. R. *Phys. Chem. Chem. Phys.* **2008**, *10*, 1177−1191.
(49) Karotki, A.; Drobizhev, M.; Kruk, M.; Spangler, C.; Nickel, E.; Mamardashvili, N.; Rebane, A. *J. Opt. Soc. Am. B* **2003**, *20*, 321−332.
(50) Arnbjerg, J.; Jiménez-Banzo, A.; Paterson, M. J.; Nonell, S.; Borrell, J. I.; Christiansen, O.; Ogilby, P. R. *J. Am. Chem. Soc.* **2007**, *129*, 5188−5199.
(51) Crank, J. *The Mathematics of Diffusion*, 2nd ed.; Oxford University Press: Oxford, U.K., 1975.
(52) Atkins, P.; de Paula, J. *Physical Chemistry*, 8th ed.; Oxford University Press: Oxford, U.K., 2006.
(53) Tsushima, M.; Tokuda, K.; Ohsaka, T. *Anal. Chem.* **1994**, *66*, 4551−4556.
(54) Hatz, S.; Poulsen, L.; Ogilby, P. R. *Photochem. Photobiol.* **2008**, *84*, 1284−1290.
(55) Born, M.; Wolf, E. *Principles of Optics*, 7th ed.; Cambridge University Press: Cambridge, U.K., 1999.
(56) Häcker, G. *Cell Tissue Res.* **2000**, *301*, 5−17.
(57) Rello, S.; Stockert, J. C.; Moreno, V.; Gámez, A.; Pacheco, M.; Juarranz, A.; Cañete, M.; Villanueva, A. *Apoptosis* **2005**, *10*, 201−208.
(58) Haugland, R. P. *Handbook of Fluorescent Probes and Research Products*, 9th ed.; Molecular Probes, Inc.: Eugene, OR, 2002.
(59) Bossy-Wetzel, E.; Green, D. R. *Methods Enzymol.* **2000**, *322*, 15−18.
(60) Engeland, M. V.; Nieland, L. J. W.; Ramaekers, F. C. S.; Schutte, B.; Reutelingsperger, C. P. M. *Cytometry* **1998**, *31*, 1−9.
(61) Niu, G.; Chen, X. *J. Nucl. Med.* **2010**, *51*, 1659−1662.
(62) Balasubramanian, K.; Bevers, E. M.; Willems, G. M.; Schroit, A. J. *Biochemistry* **2001**, *40*, 8672−8676.
(63) Davies, M. J. *Biochem. Biophys. Res. Commun.* **2003**, *305*, 761−770.
(64) Davies, M. J. *Photochem. Photobiol. Sci.* **2004**, *3*, 17−25.
(65) Alberts, B.; Johnson, A.; Lewis, J.; Raff, M.; Roberts, K.; Walter, P. *Mol. Biol. Cell*; Garland Science: New York, 2002.
(66) Kuimova, M. K.; Yahioglu, G.; Ogilby, P. R. *J. Am. Chem. Soc.* **2009**, *131*, 332−340.
(67) Soughayer, J. S.; Krasieva, T.; Jacobson, S. C.; Ramsey, J. M.; Tromberg, B. J.; Allbritton, N. L. *Anal. Chem.* **2000**, *72*, 1342−1347.
(68) Schneckenburger, H.; Hendinger, A.; Sailer, R.; Strauss, W. S. L.; Schmitt, M. *J. Biomed. Optics* **2002**, *7*, 410−416.
(69) Hell, S. W. *Science* **2007**, *316*, 1153−1158.
(70) Snyder, J. W.; Gao, Z.; Ogilby, P. R. *Rev. Sci. Instrum.* **2005**, *76*, 013701.
(71) Inoue, S.; Spring, K. R. *Video Microscopy*, 2nd ed.; Plenum: New York, 1997.
(72) *Handbook of Biological Confocal Microscopy*, 3rd ed.; Pawley, J. B., Ed.; Springer: New York, 2006.
(73) Gigler, A.; Holzwarth, M.; Marti, O. *J. Phys.: Conf. Ser.* **2007**, *61*, 780−784.